Electric-field induced ferromagnetic phase in paraelectric antiferromagnets

Maya D. Glinchuk,[1] Eugene A. Eliseev,[1] Yijia Gu,[2] Long-Qing Chen,[2] Venkatraman Gopalan,[2,*] and Anna N. Morozovska[1,3,†]

[1]*Institute for Problems of Materials Science, NAS of Ukraine, Krjijanovskogo 3, 03142 Kiev, Ukraine*

[2]*Department of Materials Science and Engineering, Pennsylvania State University, University Park, Pennsylvania 16802, USA*

[3]*Institute of Physics, NAS of Ukraine, 46, pr. Nauki, 03028 Kiev, Ukraine*

(Received 30 July 2013; revised manuscript received 10 January 2014; published 31 January 2014)

The phase diagram of a quantum paraelectric antiferromagnet $EuTiO_3$ under an external electric field is calculated using Landau-Ginzburg-Devonshire theory. The application of an electric field E in the absence of strain leads to the appearance of a ferromagnetic (FM) phase due to the magnetoelectric (ME) coupling. At an electric field greater than a critical field, E_{cr}, the antiferromagnetic (AFM) phase disappears for all considered temperatures, and FM becomes the only stable magnetic phase. The calculated value of the critical field is close to the values reported recently by Ryan *et al.* [Nat. Commun. **4**, 1334 (2013)] for $EuTiO_3$ film under a compressive strain. The FM phase can also be induced by an E-field in other paraelectric antiferromagnetic oxides with a positive AFM-type ME coupling coefficient and a negative FM-type ME coupling coefficient. The results show the possibility of controlling multiferroicity, including the FM and AFM phases, with help of an electric field application.

DOI: 10.1103/PhysRevB.89.014112 PACS number(s): 75.85.+t

I. INTRODUCTION

The search for new multiferroic materials with large magnetoelectric (ME) coupling leads to rich new physics, in addition to exciting potential applications involving magnetic field control of the dielectric properties, as well as electric field control of magnetization [1–4]. Electric (E) field control of ferromagnetism is a hot topic for the scientists around the world because it has multiple potential applications in magnetic memory storage, sensorics, and spintronics (see, e.g., Refs. [5–7], and references therein). For the case of semiconductors with a hole-induced ferromagnetism, the influence of the E-field on the carrier properties has been considered [8–10]. In the last few years, $EuTiO_3$ has been extensively studied as a basis for discovering new multiferroics. Recently, Ryan *et al.* [7] considered the possibility of a reversible control of magnetic interactions in $EuTiO_3$ thin strained films by applying an E-field. Because of Ti displacement from its central position under the E-field, changes in the spatial overlap between the electronic orbitals of the ions, and thus the magnetic exchange coupling, are expected. In particular, the density functional theory (DFT) calculation shows that the competition between ferromagnetic (FM) and antiferromagnetic (AFM) interactions is resolved in favor of FM for paraelectric $EuTiO_3$ film on compressive substrate when the applied E-field exceeds a critical value, estimated as $E_{cr} = 0.5 \times 10^6$ V/cm. It is obvious that the mechanism proposed in Ref. [7] is based on the magnetoelectric coupling.

Bulk quantum paraelectric $EuTiO_3$ is a low-temperature antiferromagnet [1,2]. It exhibits an antiferrodistortive (AFD) transition at 281 K [11–15] and is paraelectric at all temperatures. The strained $EuTiO_3$ films, surprisingly, become a strong ferroelectric ferromagnet under epitaxial tensile strains exceeding 1% [16,17].

A lot of attention has been paid to the impact of the structural AFD order parameter (oxygen octahedron static rotations [18]) on phase diagrams, structural, polar, and magnetic properties of $EuTiO_3$, and its solid solution, $Eu_xSr_{1-x}TiO_3$, with another quantum paraelectric, $SrTiO_3$ [19]. In particular, a complex interplay between the AFD order parameter and electric polarization in tensile-strained $Eu_xSr_{1-x}TiO_3$ thin films leads to the appearance of a low-symmetry monoclinic phase with in-plane ferroelectric polarization [20]. Another important possibility in $Eu_xSr_{1-x}TiO_3$ solid solution is to control the appearance of the FM phase by changing the concentration of Sr ions. The dilution of magnetic Eu ions by nonmagnetic Sr ions might change the type of magnetic order of the Eu ions because of the different percolation thresholds for FM ($x_{cr}^F \approx 0.24$) and AFM ($x_{cr}^A \approx 0.48$) order. Hence, a FM phase may become stable at some finite concentration of Sr ions [21].

These facts motivated us to perform analytical calculations on the influence of the E-field on the $EuTiO_3$ phase diagram in the framework of Landau-Ginzburg-Devonshire (LGD) theory [22–27]. In this paper, we consider the magnetoelectric coupling [28] characteristic for $EuTiO_3$ as the main mechanism of E-field influence on the phase diagram. We analyze and compare the magnetization and antimagnetization dependence on the polarization induced by an external E-field and on the magnetoelectric coupling. Our analytical results show the possibility to control multiferroicity, including the FM and AFM phases, with an applied electric field in different paraelectric antiferromagnets under certain conditions imposed on the ME coupling coefficients.

II. ELECTRIC-FIELD INDUCED FERROMAGNETISM IN BULK $EuTiO_3$

Let us study the possibility of electric-field induced ferromagnetism in bulk $EuTiO_3$ using LGD theory. For the considered case, the LGD approach is based on the phase stability analysis of thermodynamic potential (free energy),

*Corresponding author: vxg8@psu.edu

†Corresponding author: anna.n.morozovska@gmail.com

which is a series expansion to various powers of the order parameters (polarization, magnetization, and structural order parameters). The magnetization- and polarization-dependent part of the corresponding free energy is [21,29]:

$$G_M = \int_V d^3r \begin{pmatrix} \frac{\alpha_P}{2} P_3^2 + \frac{\beta_P}{4} P_3^4 - E_3 P_3 + \frac{\alpha_M}{2} M^2 + \frac{\alpha_L}{2} L^2 + \frac{\beta_M}{4} M^4 + \frac{\beta_L}{4} L^4 \\ + \frac{\lambda}{2} L^2 M^2 + \frac{P_3^2}{2}(\eta_{FM} M^2 + \eta_{AFM} L^2) + \frac{\alpha_\Phi}{2}\Phi^2 + \frac{\beta_\Phi}{4}\Phi^4 + \frac{\xi}{2}\Phi^2 P_3^2 \end{pmatrix} \quad (1)$$

Here, P_3 is the ferroelectric polarization component, E_3 is the external electric-field component, $M^2 = M_1^2 + M_2^2 + M_3^2$ is the ferromagnetic magnetization square, and $L^2 = L_1^2 + L_2^2 + L_3^2$ is the square of the antiferromagnetic order parameter, correspondingly. The last two terms represent biquadratic ME coupling between order parameters.

The expansion coefficient α_P depends on the absolute temperature T in accordance with Barrett's law, namely, $\alpha_P(T) = \alpha_T^{(P)}(T_q^{(P)}/2)(\coth(T_q^{(P)}/2T) - \coth(T_q^{(P)}/2T_c^{(P)}))$. Here, $\alpha_T^{(P)}$ is constant, temperature $T_q^{(P)}$ is the so-called quantum vibration temperature related with polar soft modes, and $T_c^{(P)}$ is the "effective" Curie temperature corresponding to the polar modes in bulk $EuTiO_3$. Coefficient β_P is regarded as temperature independent [21].

The expansion coefficient α_M depends on the temperature in accordance with Curie's law, namely, $\alpha_M(T) = \alpha_C(T - T_C)$, where T_C is the FM Curie temperature. Note that the dependence determines the experimentally observed inverse magnetic susceptibility in the paramagnetic phase of $EuTiO_3$. The temperature dependence of the expansion coefficient α_L is $\alpha_L(T) = \alpha_N(T - T_N)$, where T_N is the Neel temperature for bulk $EuTiO_3$. For equivalent permutated magnetic Eu ions with antiparallel spin ordering, it can be assumed that $\alpha_C \approx \alpha_N$. The coefficient λ of coupling between magnetic (M) and antiferromagnetic (L) order parameters (LM-coupling) should be positive, because only the positive coupling term $\lambda L^2 M^2/2$ prevents the appearance of FM (as well as ferrimagnetic) phases at low temperatures $T < T_C$ under the condition of $\sqrt{\beta_M \beta_L} < \lambda$, regarded as valid hereafter [7]. Coefficients β_L and β_M are regarded as positive and temperature independent.

The biquadratic ME coupling contribution is $(\eta_{FM} M^2 + \eta_{AFM} L^2) P_3^2/2$. Following Lee *et al.* [17], we assume that the ME coupling coefficients of FM and AFM are equal and positive, i.e., $\eta_{AFM} \approx -\eta_{FM} > 0$ for numerical calculations, as anticipated for equivalent magnetic Eu ions with antiparallel spin ordering in bulk $EuTiO_3$.

Here, Φ is the structural order parameter (AFD displacement). The corresponding expansion coefficient α_Φ depends on the absolute temperature T in accordance with Barrett's law, $\alpha_\Phi(T) = \alpha_T^{(\Phi)}(T_q^{(\Phi)}/2)(\coth(T_q^{(\Phi)}/2T) - \coth(T_q^{(\Phi)}/2T_S))$ [11,12,19,20]. The biquadratic coupling coefficient ξ is regarded as temperature independent [30–32]. The last term in Eq. (1) describes the biquadratic coupling between the polarization and AFD order parameter. Neglecting the coupling between the (antiferro)magnetic and AFD order parameters, we utilize the fact that a strong magnetic field could shift the transition from cubic to AFD tetragonal phase in $EuTiO_3$, but the shift is rather moderate, less than 5 K, and appears only at rather a high field of 9 Tesla [33]. Hence, we can neglect the coupling between AFD and magnetization, since we aim to consider the effects associated with the application of the electric field, not the magnetic field.

Note that magnetic anisotropy should be included in the functional Eq. (1) in the general case, and it should be coupled to the elastic strain u_{kl} via the magnetoelastic coupling term, $\mu_{ijkl} M_i M_j u_{kl}$, allowed by the parent phase symmetry. Unfortunately, in the case of $EuTiO_3$, very little is known about the coupling tensor μ_{ijkl} between the magnetization vector components M_i and strain tensor u_{kl}. Following Scagnoli *et al.* [34], magnetoelastic coupling, if present, is expected to be negligible. So, restricted by the lack of experimental data about the magnetic anisotropy of $EuTiO_3$, we neglect the magnetoelastic effect in Eq. (1).

Note also, that Barret's law may have restrictions and more complex expressions should be considered in the case of several coupled order parameters [35]. Considering the case of incipient ferroelectric and in order to obtain analytical results, one could suppose a linear dependence of polarization on the applied electric field

$$P_3 \approx \chi E_3 \quad (2)$$

Here we introduce a linear dielectric susceptibility χ as

$$\chi = \frac{1}{\alpha_P + \xi\Phi^2 + \eta_{FM} M^2 + \eta_{AFM} L^2} \quad (3)$$

Note that $\alpha_P \to \alpha_P + \xi\Phi^2 + \eta_{FM} M^2 + \eta_{AFM} L^2$ in the denominator of Eq. (3) due to the AFD and ME coupling.

Equations of state for the absolute value of the magnetization M and the antimagnetization L can be obtained from the minimization of the free energy (Eq. (1)). They are $(\alpha_M + \eta_{FM} P_3^2) M + \beta_M M^3 + \lambda L^2 M = 0$ and $(\alpha_L + \eta_{AFM} P_3^2) L + \beta_L L^3 + \lambda L M^2 = 0$. The formal solution of these equations contains the possible E-field induced phase transition, namely, the appearance of the mixed FM phase with order parameters:

$$M = \sqrt{\frac{\alpha_L \lambda - \alpha_M \beta_L + (\lambda \eta_{AFM} - \beta_L \eta_{FM}) P^2}{\beta_M \beta_L - \lambda^2}} \quad (4a)$$

$$L = \sqrt{\frac{\alpha_M \lambda - \alpha_L \beta_M + (\lambda \eta_{FM} - \beta_M \eta_{AFM}) P^2}{\beta_M \beta_L - \lambda^2}} \quad (4b)$$

The critical values of polarization could be found by substituting into the equations either $M = 0$ or $L = 0$, i.e.,

$$P_{cr}|_{M=0} = \sqrt{\frac{\alpha_M \beta_L - \alpha_L \lambda}{\lambda \eta_{AFM} - \beta_L \eta_{FM}}},$$

$$P_{cr}|_{L=0} = \sqrt{\frac{\alpha_L \beta_M - \alpha_M \lambda}{\lambda \eta_{FM} - \beta_M \eta_{AFM}}}. \quad (5)$$

The expressions in Eq. (5) correspond to the lower and upper critical fields, respectively:

$$E_{cr}|_{M=0} = \frac{1}{\chi}\sqrt{\frac{\alpha_M\beta_L - \alpha_L\lambda}{\lambda\eta_{AFM} - \beta_L\eta_{FM}}},$$
$$E_{cr}|_{L=0} = \frac{1}{\chi}\sqrt{\frac{\alpha_L\beta_M - \alpha_M\lambda}{\lambda\eta_{FM} - \beta_M\eta_{AFM}}} \quad (6)$$

Note, that the LM-coupling constant λ, β_M, and β_L are positive, as required for the stability of free energy (Eq. (1)). Using the conditions in the expressions in Eq. (6), the conditions $\eta_{FM} < 0$, $\eta_{AFM} > 0$, $\alpha_M(T) > 0$, and $\alpha_L(T) < 0$ are sufficient for the absolute stability of the FM phase at applied electric fields greater than the critical field $E_{cr}|_{M=0}$, and with arbitrary positive values of λ and $\beta_{L,M}$. Note, that under the typical condition of small positive LM-coupling constant λ, one immediately obtains from Eq. (6), simpler equations $E_{cr}|_{M=0} \approx \chi^{-1}\sqrt{-\alpha_M/\eta_{FM}}$ and $E_{cr}|_{L=0} \approx \chi^{-1}\sqrt{-\alpha_L/\eta_{AFM}}$ that are useful for estimations.

Using the free energy (Eq. (1)) with $EuTiO_3$ parameters listed in Table I, one could see that the condition $E > E_{cr}|_{M=0}$ becomes valid for electric fields greater than 480 kV/cm at 0 K. The value is in reasonable agreement with DFT simulations performed by Ryan *et al.* [7].

The complex behavior of M and L induced by E_3 can be explained by the phase diagram of bulk $EuTiO_3$ in the coordinates of temperature and external electric field, as shown in Figure 1(a). Note that all the magnetic phases also possess an AFD ordering, and the influence is evidently included in the LGD-expansion (Eq. (1)); corresponding coefficients are listed in Table I. One can see from the diagram that the FM phase stability region starts at electric fields greater than 0.5 MV/cm at 0 K and converges to 0.83 MV/cm at 4 K. The paramagnetic (PM) phase is stable at temperatures greater than 5 K, while its boundary with the AFM phase slightly shifts to lower temperatures as the electric field increases. A triangular-like region of the AFM phase exists between the FM and PM phases at temperatures lower than 5 K and electric fields less than 0.83 MV/cm. A rather thin wedge-like region of the ferrimagnetic (FI) phase exists between the FM and AFM phases at temperatures less than 3 K and for fields between 0.4 MV/cm and 0.7 MV/cm. At a field of $E_{cr} \geqslant 0.83$ MV/cm, the AFM phase disappears at all considered temperatures, and so the true FM phase becomes the only absolutely stable magnetic phase. The phase diagram proves that an electric field higher than E_{cr} transforms the bulk $EuTiO_3$ into a true and relatively strong FM state at temperatures lower than 5 K. The result opens up the possibility to control bulk $EuTiO_3$ between different magnetic phases using an external electric field. In particular, our calculations prove that it becomes possible to control the multiferroicity, including the content of FM and AFM phases, with the help of external electric fields. Note that Fig. 1(a) addresses the question of which phase (FM, FI, AFM, or PM) is absolutely stable at a given temperature and electric field.

Figure 1(b) illustrates the temperature dependencies of the magnetization M (solid curves) and antimagnetization L (dashed curves) for different values of external electric field. Mostly, there are regions where both M and L coexist,

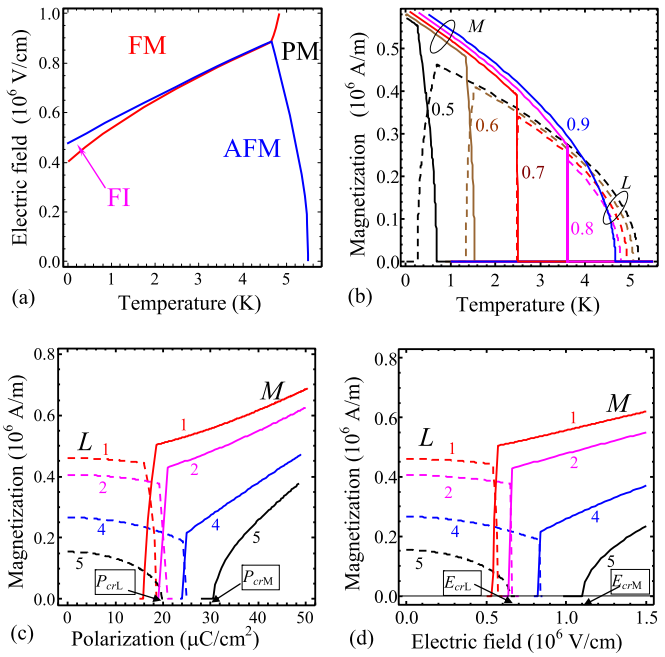

FIG. 1. (Color online) Electric-field control of bulk $EuTiO_3$ magnetic properties. (a) Phase diagram of bulk $EuTiO_3$ in the coordinates of temperature versus external electric field. Abbreviations PM, FI, FM, and AFM denote paramagnetic, ferrimagnetic, ferromagnetic, and antiferromagnetic phases, respectively. (b) Temperature dependencies of the magnetization M (solid curves) and antimagnetization L (dashed curves) for different values of external electric field E_3 = 0.5, 0.6, 0.7, 0.8, and 0.9 MV/cm (numbers near the curves). (c,d) Magnetization M (solid curves) and antimagnetization L (dashed curves) as a function of polarization (c) and induced by an external electric field (d) at different temperatures of 1, 2, 4, and 5 K (numbers near the curves).

indicating the presence of an electric-field induced FI phase that microscopically could be realized as a canted AFM phase, as anticipated for equivalent magnetic Eu ions with antiparallel spin ordering at zero field. For realistic values of applied field, the temperature range of the FM phase is below 5 K. As one can see from Fig. 1(b), the temperature interval for the existence of magnetization M increases with applied electric field. For example, the transition to FM phase occurs at 1 K for the field E_3 = 0.5 MV/cm and at 5 K for E_3 = 0.9 MV/cm. Note that the FM transition is of the second order for E_3 = 0.9 MV/cm, but it is more close to the first order at smaller E_3. The magnetization value, which is ~0.5 A/m at low temperatures, is higher than the corresponding antimagnetization. Antimagnetization, L, completely disappears for E_3 = 0.83 MV/cm, and only FM magnetization exists at this field. Antimagnetization L disappears at about 5 K and electric field E_{crL} = 0.65 MV/cm (the second-order phase transition). The points of the second-order phase transition depend on the E_3 value rather weakly. In contrast to magnetization, which appears at low temperatures at E-field higher than critical one and then only increases as the temperature decreases down to 0 K, the antimagnetization L does not exist at low temperatures and at E-field higher than critical one it typically appears in the temperature range with no magnetization

TABLE I. Expansion coefficients of the LGD free energy from Eq. (1) for bulk $EuTiO_3$. Polarization-related coefficients have indexes "P", magnetization and antimagnetization coefficients have indexes "M" and "L" correspondingly, and AFD order parameter–related coefficients have indexes "Φ". ΦP-, LM-, and ME-coupling coefficients are listed in the last lines of the table. Note, the equality $\alpha_C \approx \alpha_N$ comes from the equivalence of the magnetic sublattices in $EuTiO_3$.

Coefficient	SI units	Value
Coefficient before P^2, $\alpha_P(T) = \alpha_T^{(P)}(T_q^{(P)}/2)(\coth(T_q^{(P)}/2T) - \coth(T_q^{(P)}/2T_c^{(P)}))$		
Inverse dielectric stiffness constant, $\alpha_T^{(P)}$	10^6 m/(F K)	1.95
Effective Curie temperature $T_c^{(P)}$	K	−133.5
Characteristic temperature $T_q^{(P)}$	K	230
Coefficient before P^4, β_P	10^9 m^5/(C^{2}F)	1.6
Coefficient before M^2, $\alpha_M(T) = \alpha_C(T - T_C)$		
Inverse Curie constant, α_C	Henri/(m·K)	$2\pi\cdot10^{-6}$
FM Curie temperature, T_C	K	3.5 ± 0.3
Coefficient before M^4, β_M	J m/A^4	0.8×10^{-16}
Coefficient before L^2, $\alpha_L(T) = \alpha_N(T - T_N)$		
Inverse Neel constant, α_N	Henri/(m·K)	$2\pi\cdot10^{-6}$
AFM Neel temperature, T_N	K	5.5
Coefficient before L^4, β_L	J m/A^4	1.33×10^{-16}
Coefficient before Φ^2, $\alpha_\Phi(T) = \alpha_T^{(\Phi)}(T_q^{(\Phi)}/2)(\coth(T_q^{(\Phi)}/2T) - \coth(T_q^{(\Phi)}/2T_S))$		
Coefficient $\alpha_T^{(\Phi)}$	J/(m^5 K)	3.91×10^{26}
Characteristic temperature $T_q^{(\Phi)}$	K	205
AFD transition temperature T_S	K	270
Coefficient before Φ^4, β_Φ	J/m^7	0.436×10^{50}
ΦP-coupling coefficient ξ	(F m)$^{-1}$	-2.225×10^{29}
LM-coupling coefficient λ	J m/A^4	1.0×10^{-16}
ME-coupling coefficient η_{AFM}	J m^3/(C^2 A^2)	8×10^{-5}
ME-coupling coefficient η_{FM}	J m^3/(C^2 A^2)	-8×10^{-5}

(compare solid and dashed curves in Fig. 1(b)). The higher the electric field, the smaller is the temperature region of nonzero antimagnetization: For example, it exists from 0.5 K to 5 K at $E_3 = 0.5$ MV/cm and from 3.5 K to 4.5 K at $E_3 = 0.9$ MV/cm.

Figures 1(c) and 1(d) illustrate magnetization M (solid curves) and antimagnetization L (dashed curves) as a function of polarization induced by an external electric field and as a function of electric field itself at different temperatures from 1 to 5 K. One can see that at electric fields less than the critical value, only AFM magnetization exists. For the electric fields greater than the critical value, a ferromagnetic magnetization occurs and increases as the strength of the electric field (or polarization) increases. An unusual cross-over from the first-order phase transition (corresponding to the FM magnetization appearance) to a second-order transition appears with an increase in temperature. The decrease in antimagnetization for electric fields greater than the critical value follows the first-order transition. The critical field value increases, and the "gap" between the AFM and FM states shrinks as the temperature increases (compare the curves calculated for 1 K with the ones for 4 K). At temperatures of 1–4 K, the thin region of M and L coexistence, i.e., FI phase, is seen. At 5 K, there is a pronounced gap between the AFM and FM states.

Note that the critical values of polarization and E-field depend on the temperature, as one can see from the examples shown in Figs. 1(c) and 1(d). A comparison of the x-axis in Figs. 1(c) and 1(d) provides insight into the polarization values induced by the electric field. Polarization below P_{cr} (or subcritical electric fields) cannot induce the FM in bulk $EuTiO_3$. At the same time, a polarization value higher than the critical value induces FM with rather high M values (up to 0.6 MA/m). The LGD approach makes it possible to calculate the corresponding phase diagram of the dependence of stable magnetic phases on the applied electric field and magnetoelectric characteristics.

Although the main result of the study is that strain is not required to realize the FM phase, the value of the critical electric field should change with the strain. We can expect different trends for the value of critical field under the application of hydrostatic pressure or biaxial tensile or compressive strains to $EuTiO_3$. Our estimations show that the critical electric field should increase under hydrostatic pressure, while it can change in an anisotropic manner for biaxial tensile or compressive strains. Biaxial strains can lead to an increase in the critical field in some direction and a decrease in the other directions. The impact of shear strains can be even more complex.

III. DISCUSSION AND CONCLUSION

The phase diagram proves that an electric field higher than E_{cr} transforms the bulk $EuTiO_3$ into a true and relatively strong FM state at temperatures lower 5 K. Therefore, it can be shown that at fields E greater than $E_{cr} = 0.83$ MV/cm and temperatures $T < 5$ K, the transition temperature to the FM phase becomes higher than the transition temperature to the

TABLE II. Critical electric fields calculated at zero temperature for several paraelectric antiferromagnets. To calculate the critical fields, we used Neel temperature, dielectric susceptibility, and ME-coupling coefficients also listed in the table. Note the spin-phonon coupling in $Sr_{1-x}Ba_xMnO_3$ ($x = 0.3$) is more than 500 times stronger than that for $EuTiO_3$.

Paraelectric antiferromagnet	Neel temperature T_N (K)	Dielectric susceptibility at 0 K	ME-coupling coefficients (J m^3/[C^2 A^2])	Critical field at 0 K	Ref.
(V/cm)					
$Sr_{1-x}Ba_xMnO_3$					
($x = 0.3$)	215	≈400	$\eta_{AFM} = -\eta_{FM} = 4 \times 10^{-2}$	0.2×10^5	[36,38]
$EuTiO_3$	5.5	390	$\eta_{AFM} = -\eta_{FM} = 8 \times 10^{-5}$	0.4×10^6	Table I
$MnTiO_3$	65	$\chi^{\parallel} = 21$	$\eta^{\parallel}_{FM} = 0.47$, $\eta^{\perp}_{FM} = 0.18$	Does not exist	[39,40]
		$\chi^{\perp} = 38$	η_{AFM} = not found	because $\eta_{FM} > 0$	

AFM phase. Allowing for the possibility that the value of the transition temperature will depend on the superexchange of Eu-Ti-Eu bond alignment and on the degree of interatomic orbital overlap, the distortion induced by an electric field could significantly alter the magnetic structure of the entire system. Such behavior follows from Figs. 1(c) and 1(d), where the dependence of magnetization and antimagnetization on polarization and electric field is presented for several temperatures. Also from Figs. 1(c) and 1(d), one can see that the magnetization increases as the polarization increases, while the antimagnetization decreases. Thus, the shift of Ti ions from the central position induced by the electric field disrupts the long-range spin coherence of the AFM order originating from the interaction with third Eu ion neighbors, while the first and the second neighboring Eu ions are ferromagnetically ordered in accordance with the results of Ryan *et al.* [7].

Generally speaking, one can look for the fulfilment of expressions in Eq. (6) in other paraelectric antiferromagnetic oxides with ME coupling coefficients satisfying the conditions $\eta_{FM} < 0$ and $\eta_{AFM} > 0$, where the magnetization could be induced by an electric field $E > E_{cr}|_{M=0}$ (where $E_{cr}|_{M=0}$ is given by Eq. (6)), at some temperature range defined by the conditions $\alpha_M(T) > 0$ and $\alpha_L(T) < 0$. The search for such materials seems to be important both for understanding the mechanisms of ME coupling and for possible applications. The main current problem is the limited knowledge about ME coupling coefficients.

Let us discuss some cases when one can expect E-field induced magnetization. In particular, such supposition can be made on the basis of data known for solid solutions $Sr_{1-x}Ba_xMnO_3$ [36] and $Sr_{1-x}Eu_xTiO_3$ [21]. Sakai *et al.* [36] has shown the strong suppression of ferroelectricity observed at $x \geqslant 0.4$ and originated from displacement of Mn^{+4} ions upon the AFM order. This gives direct evidence that $\eta_{AFM} > 0$, and with respect to the above written expression for the critical field, $\eta_{FM} < 0$. The assumption about different signs of η_{FM} and η_{AFM} also agrees with Smolenskii and Chupis [37], as well as Katsufuji [1] and Lee *et al.* [17]. In particular, Smolenskii and Chupis and Katsufuji [1] stated that it is natural to consider that the dielectric constant is dominated by the pair correlation between the nearest spins, which phenomenologically leads to the ME term $\eta P^2(M^2 - L^2)$. Therefore, we arrive at the conclusion about the fulfilment of conditions in Eq. (6) and hence the possibility to induce magnetization by E-field at $x < 0.4$, e.g., $x = 0.2$, where we have a paraelectric antiferromagnet. Following Table II, we calculated the critical E-field for $Sr_{0.7}Ba_{0.3}MnO_3$, which is equal to 0.2×10^5 V/cm at 0 K.

Another solid solution (Eu,Sr)TiO_3 considered by us [21] could have ME characteristics $\eta_{FM} < 0$ and $\eta_{AFM} > 0$ (see Table I). Since it is possible to have a FM phase for x between the percolation thresholds of the FM ($x = 0.24$) and AFM phases ($x = 0.48$) [21], one has to look for the E-field induced FM phase, e.g., at $x < 0.2$.

Note that in Table II, we did not include the already mentioned $E_{cr} = 0.5 \times 10^6$ V/cm for $EuTiO_3$ film under biaxial compressive strain [17] and the $Sr_xEu_{1-x}TiO_3$ paraelectric antiferromagnet for $x < 0.2$, since we do not know the values for all the necessary parameters. The search for other paraelectric antiferromagnets that satisfy the conditions $\eta_{FM} < 0$ and $\eta_{AFM} > 0$ is in progress.

An experimental confirmation of the theoretical prediction is desirable. The observation of the FM phase under an electric field or induced by polarization due to a shift in Mn^{+4} or Ti^{+4} ions will provide direct evidence of the magnetoelectric coupling mechanism based on the superexchange of Mn-O-Mn or Eu-Ti-Eu bonds proposed recently in Refs. [7,36] based on first principle calculations.

Ryan *et al.* [7] proposed to use the electric field to tune the magnetism in strained $EuTiO_3$ *thin film*. Note that *elastic strain* has been a critical component for inducing ferroelectricity with ferromagnetism in $EuTiO_3$ thin films. In contrast, in this study, we predict that this coupling is also possible in *bulk unstrained* $EuTiO_3$ and in other paraelectric antiferromagnet oxides with a positive AFM-type magnetoelectric coupling coefficient and a negative FM-type magnetoelectric coupling coefficient. Since the coupling coefficients, including their signs, are defined by the microscopic interactions, we believe that our predictions indeed reflect the underlying physical mechanism of the phenomena. The critical electric field required for the origin of ferromagnetism varies from relatively high values, 0.83 MV/cm (for bulk $EuTiO_3$), to relatively small values, 0.02 MV/cm (for bulk $Sr_{0.7}Ba_{0.3}MnO_3$). We hope that our phenomenological prediction can stimulate systematic *ab initio* calculations and experimental studies of the couplings in paraelectric antiferromagnet oxides.

ACKNOWLEDGMENTS

The authors acknowledge financial support from the US National Science Foundation (NSF), under

Grant No. DMR-1210588 and No. DMR-0820404, and State Fund of Fundamental Research of Ukraine (SFFR), Grant No. UU48/002, via a bilateral SFFR-NSF project.

[1] T. Katsufuji and H. Takagi, Phys. Rev. B **64**, 054415 (2001).
[2] V. V. Shvartsman, P. Borisov, W. Kleemann, S. Kamba, and T. Katsufuji, Phys. Rev. B **81**, 064426 (2010).
[3] M. Fiebig, J. Phys. D: Appl. Phys. **38**, R123 (2005).
[4] Yurong Yang, Wei Ren, Massimiliano Stengel, X. H. Yan, and L. Bellaiche, Phys. Rev. Lett. **109**, 057602 (2012).
[5] S. M. Wu, Shane A. Cybart, P. Yu, M. D. Rossell, J. X. Zhang, R. Ramesh, and R. C. Dynes, Nat. Mater. **9**, 756 (2010).
[6] Y. Tokunaga, Y. Taguchi, T.-H. Arima, and Y. Tokura, Nat. Phys. **8**, 838 (2012).
[7] P. J. Ryan, J.-W. Kim, T. Birol, P. Thompson, J.-H. Lee, X. Ke, P. S. Normile, E. Karapetrova, P. Schiffer, S. D. Brown, C. J. Fennie, and D. G. Schlom, Nat. Commun. **4**, 1334 (2013).
[8] H. Ohno, D. Chiba, F. Matsukura, T. Omiya, E. Abe, T. Dietl, Y. Ohno, and K. Ohtani, Lett. Nature **408**, 944 (2000).
[9] T. Lottermoser, T. Lonkai, Uwe Amann, D. Hohlwein, J. Ihringer, and Manfred Fiebig, Nature **430**, 541 (2004).
[10] D. Chiba, M. Sawicki, Y. Nishitani, Y. Nakatani, F. Matsukura, and H. Ohno, Nat. Lett. **455**, 515 (2008).
[11] A. Bussmann-Holder, J. Kohler, R. K. Kremer, and J. M. Law, Phys. Rev. B **83**, 212102 (2011).
[12] M. Allieta, M. Scavini, L. J. Spalek, V. Scagnoli, H. C. Walker, C. Panagopoulos, S. S. Saxena, T. Katsufuji, and C. Mazzoli, Phys. Rev. B **85**, 184107 (2012).
[13] K. Z. Rushchanskii, N. A. Spaldin, and M. Lezaic, Phys. Rev. B **85**, 104109 (2012).
[14] V. Goian, S. Kamba, O. Pacherova, J. Drahokoupil, L. Palatinus, M. Dusek, J. Rohlıcek, M. Savinov, F. Laufek, W. Schranz, A. Fuith, M. Kachlık, K. Maca, A. Shkabko, L. Sagarna, A. Weidenkaff, and A. A. Belik, Phys. Rev. B **86**, 054112 (2012).
[15] A. P. Petrovic, Y. Kato, S. S. Sunku, T. Ito, P. Sengupta, L. Spalek, M. Shimuta, T. Katsufuji, C. D. Batista, S. S. Saxena, and C. Panagopoulos, Phys. Rev. B **87**, 064103 (2013).
[16] C. J. Fennie and K. M. Rabe, Phys. Rev. Lett. **97**, 267602 (2006).
[17] J. H. Lee, L. Fang, E. Vlahos, X. Ke, Y. Woo Jung, L. F. Kourkoutis, Jong-Woo Kim, P. J. Ryan, Tassilo Heeg, M. Roeckerath, V. Goian, M. Bernhagen, R. Uecker, P. C. Hammel, K. M. Rabe, S. Kamba, J. Schubert, J. W. Freeland, D. A. Muller, C. J. Fennie, P. Schiffer, V. Gopalan, E. Johnston-Halperin, and D. Schlom, Nature (London) **466**, 954 (2010).
[18] Yijia Gu, Karin Rabe, Eric Bousquet, Venkatraman Gopalan, and Long-Qing Chen, Phys. Rev. B **85**, 064117 (2012).
[19] Z. Guguchia, A. Shengelaya, H. Keller, J. Kohler, and A. Bussmann-Holder, Phys. Rev. B **85**, 134113 (2012).
[20] A. N. Morozovska, Y. Gu, V. V. Khist, M. D. Glinchuk, L.-Q. Chen, V. Gopalan, and E. A. Eliseev, Phys. Rev. B **87**, 134102 (2013).
[21] E. A. Eliseev, M. D. Glinchuk, V. V. Khist, C.-W. Lee, C. S. Deo, R. K. Behera, and A. N. Morozovska, J. Appl. Phys. **113**, 024107 (2013).
[22] A. N. Morozovska, E. A. Eliseev, and M. D. Glinchuk, Phys. Rev. B **73**, 214106 (2006).
[23] A. N. Morozovska, M. D. Glinchuk, and E. A. Eliseev, Phys. Rev. B **76**, 014102 (2007).
[24] Ji Zang, Minghuang Huang, and Feng Liu, Phys. Rev. Lett. **98**, 146102 (2007).
[25] Ji Zang and Feng Liu, Nanotechnology **18**, 405501 (2007).
[26] S. P. Lin, Yue Zheng, M. Q. Cai, and Biao Wang, Appl. Phys. Lett. **96**, 232904 (2010).
[27] Yue Zheng and C. H. Woo, J. Appl. Phys. **107**, 104120 (2010).
[28] M. D. Glinchuk, E. A. Eliseev, A. N. Morozovska, and R. Blinc, Phys. Rev. B **77**, 024106 (2008).
[29] A. N. Morozovska, M. D. Glinchuk, R. K. Behera, B. Y. Zaulychny, C. S. Deo, and E. A. Eliseev, Phys. Rev. B **84**, 205403 (2011).
[30] A. K. Tagantsev, E. Courtens, and L. Arzel, Phys. Rev. B, **64**, 224107 (2001).
[31] M. J. Haun, E. Furman, T. R. Halemane and L. E. Cross, Ferroelectrics **99**, 55 (1989); **99**, 13 (1989),
[32] B. Houchmandzadeh, J. Lajzerowicz, and E. Salje, J. Phys.: Condens. Matter **3**, 5163 (1991).
[33] Z. Guguchia, H. Keller, J. Köhler, and A. Bussmann-Holder, J. Phys.: Condens. Matter **24**, 492201 (2012).
[34] Valerio Scagnoli, Mattia Allieta, Helen Walker, Marco Scavini, Takuro Katsufuji, Leyre Sagarna, Oksana Zaharko, and Claudio Mazzoli, Phys. Rev. B **86**, 094432 (2012).
[35] J. M. Pérez-Mato and E. K. H. Salje, Philos. Mag. Lett., **81**, 885 (2001).
[36] H. Sakai, J. Fujioka, T. Fukuda, D. Okuyama, D. Hashizume, F. Kagawa, H. Nakao, Y. Murakami, T. Arima, A. Q. R. Baron, Y. Taguchi, and Y. Tokura, Phys. Rev. Lett. **107**, 137601 (2011).
[37] G. A. Smolenskiĭ and I. E. Chupis. Sov. Phys. Usp. **25**, 475 (1982).
[38] H. Sakai, J. Fujioka, T. Fukuda, M. S. Bahramy, D. Okuyama, R. Arita, T. Arima, A. Q. R. Baron, Y. Taguchi, and Y. Tokura, Phys. Rev. B **86**, 104407 (2012).
[39] John J. Stickler, S. Kern, A. Wold, and G. S. Heller, Phys. Rev. **164**, 765 (1967).
[40] N. Mufti, G. R. Blake, M. Mostovoy, S. Riyadi, A. A. Nugroho, and T. T. M. Palstra, Phys. Rev. B **83**, 104416 (2011).